Underwater acoustic passive localization base on multipath arrival structure

Liang AN[1]; Lijun CHEN[2]

[1, 2] Southeast University, China

ABSTRACT

An acoustic passive localization method for underwater targets in shallow water waveguide using homomorphic signal processing is presented in this paper. The multipath arrival structure is extracted from source radiated noise by cepstrum analysis. Instead of using the single reflection path, the source range and depth are estimated by the time-delay differences between direct path and twice reflection paths, such as surface-bottom reflection path and bottom-surface reflection path. The estimation performance is analyzed with computer simulation in an ideal waveguide. BELLHOP model is used to examine the effect of ray warping on the localization method in Pekeris waveguide and real ocean waveguide.

Keywords: Multipath, Localization, Cepstrum   I-INCE Classification of Subjects Number(s): 74.5

1. INTRODUCTION

Passive localization using a single hydrophone or small-aperture array is a difficult problem in underwater acoustics. Classical passive localization methods such as matched filed processing (1, 2), range differences (3) and target motion analysis (4, 5) are unsuitable with single hydrophone configuration.

The passive localization methods by single hydrophone have already been studied since 1990s. Generally, there are two types of methods. One is the matched filed processing (including matched mode processing). Another is the time delays matching. Lee used the measured impulse response of the environmental and MFP (matched filed processing) to localize a source transmitting M-sequence pulse (6). Touz´e et al performed source localization in depth and range using a single hydrophone by incoherent and coherent MFP (7). Jesus et al estimated the subspace spanned by the delayed source signal paths and localized the source using a family of measures of the distance between that subspace and the subspace spanned by the replicas provided by the model (8). Tao et al proposed a method that involved only processing the intensity surface of the spectrogram of received broadband acoustic signals and estimated the motion parameters by the principle of the waveguide invariant theory (9).

In this paper, a new passive acoustic localization method with single hydrophone configuration is proposed. The source range and depth are estimated by the time-delay difference between direct path and twice reflection paths, such as surface-bottom reflection path and bottom-surface reflection path. The estimator has analytical expressions of source range and depth as well as small calculating amount.

2. LOCALIZATION METHOD

2.1 Theory

In shallow-water channels, multipath is caused by multiple reflections of the ocean's surface and bottom. Wu derived the formula of source range and depth estimation using surface and bottom delay (10). Consider three paths case, the radiated noise propagates through direct-path, surface reflection path and bottom reflection path to a hydrophone as shown in Figure 1. T is the sound source, and R is the hydrophone. The ranges of the direct path, surface reflection path and bottom reflection path are R_d,

[1] anliang@seu.edu.cn

[2] ljchen@seu.edu.cn

R_s and R_b respectively. H_t is the depth of the sound source and H_r is the depth of the hydrophone. H_S is the depth of the sea. R_1 is the surface mirror image of the R, while R_2 is the bottom mirror image of R. α is the grazing angle and we suppose that

$$\begin{cases} \alpha > 0, & \text{when } H_t < H_r \\ \alpha = 0, & \text{when } H_t = H_r \\ \alpha < 0, & \text{when } H_t > H_r \end{cases}$$

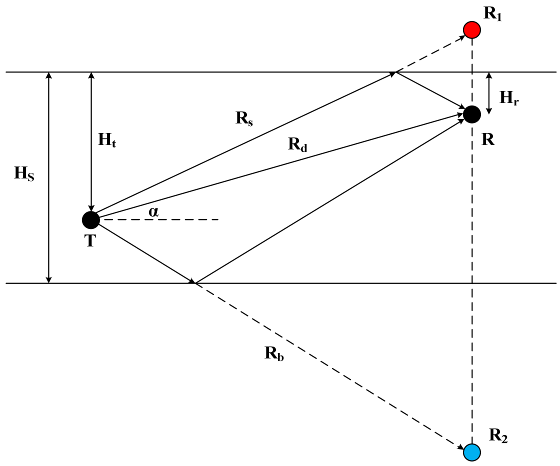

Figure 1 – Geometry of single-reflection paths

From simple geometrical relationship, the acoustic range of the surface reflection path and bottom reflection path could be written as Eq.(1) and Eq.(2).

$$R_s = R_d + c\tau_1 \tag{1}$$

$$R_b = R_d + c\tau_2 \tag{2}$$

Where, τ_1 is the time delay difference between surface path and direct path, τ_2 is the time delay difference between bottom path and direct path and c is the sound speed in water. By using cosine theorem, R_s and R_b could also be written as Eq.(3) and Eq.(4),

$$R_s^2 = R_d^2 + D_1^2 - 2R_d D_1 \cos\left(\frac{\pi}{2} - \alpha\right) \tag{3}$$

$$R_b^2 = R_d^2 + D_2^2 - 2R_d D_2 \cos\left(\frac{\pi}{2} + \alpha\right) \tag{4}$$

where

$$D_1 = 2H_r \tag{5}$$

$$D_2 = 2(H_s - H_r) \tag{6}$$

Put Eq.(1) and Eq.(2) into Eq.(3) and Eq.(4), we have

$$2R_d c\tau_1 + c^2\tau_1^2 = D_1^2 - 2R_d D_1 \sin\alpha \tag{7}$$

$$2R_d c\tau_2 + c^2\tau_2^2 = D_2^2 + 2R_d D_2 \sin\alpha \tag{8}$$

By solving Eq.(7) and Eq.(8), R_d and H_t could be estimated by Eq.(9) and Eq.(10). This method is called DSB method in this paper.

$$R_d = \frac{D_1 D_2 (D_1 + D_2) - c^2 (D_1\tau_2^2 + D_2\tau_1^2)}{2c(D_1\tau_2 + D_2\tau_1)} \tag{9}$$

$$H_t = \frac{D_2\tau_1 (D_1 + D_2) - c^2 \tau_1\tau_2 (\tau_2 - \tau_1)}{2(D_1\tau_2 + D_2\tau_1)} \tag{10}$$

From Eq.(9) and Eq.(10), the source range and depth could be estimated simultaneously by using two single-reflection paths. But with the source range increasing, the two single-reflection paths would become unstable and even vanish. In these situations, another method must be found to estimate the source range and depth. The geometry of twice-reflection paths is shown in Figure 2. R_1 is the surface mirror image of the R, R_2 is the bottom mirror image of R, R_3 is the bottom mirror image of R_1 and R_4 is the surface mirror image of R_2. Here, R_{sb} is the surface-bottom path and R_{bs} is the bottom-surface path. R_{sb} and R_{bs} are all twice-reflection paths, which interact with the boundaries twice.

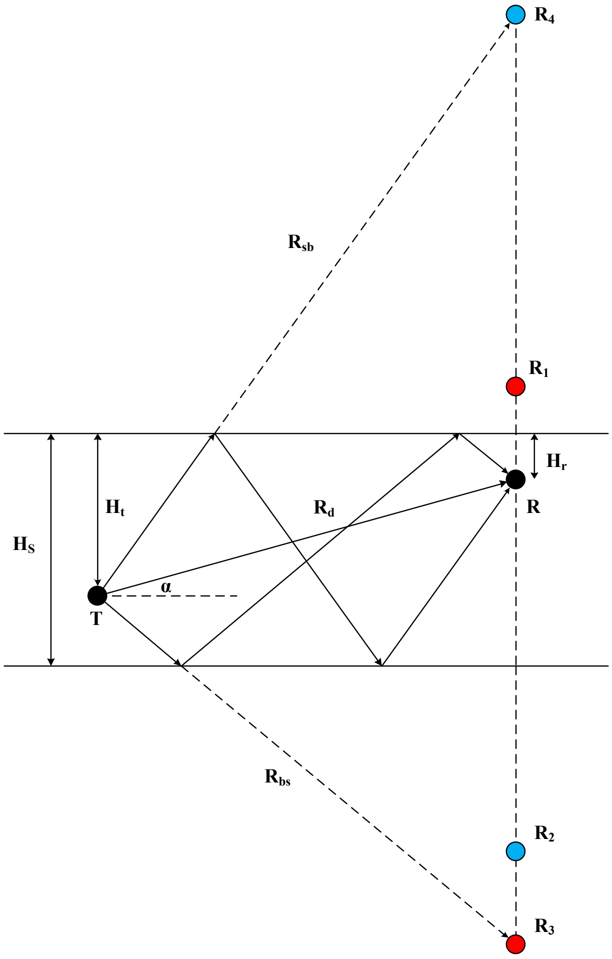

Figure 2 – Geometry of twice-reflection paths

Similarly, some equations could be established from geometrical relationship as shown from Eq.(11) to Eq.(16).

$$R_{sb} - R_d = c\tau_3 \tag{11}$$

$$R_{bs} - R_d = c\tau_4 \tag{12}$$

$$R_{sb}^2 = H_h^2 + (2H_S - H_r + H_t)^2 \tag{13}$$

$$R_{bs}^2 = H_h^2 + (2H_S + H_r - H_t)^2 \tag{14}$$

$$H_h = R_d \cos\alpha \tag{15}$$

$$H_t = H_r - R_d \sin\alpha \tag{16}$$

Where, τ_3 is the time delay difference between surface-bottom path and direct path, τ_4 is the time delay difference between bottom-surface path and direct path. Plus the square of Eq.(11) and the square of Eq.(12), we could have Eq.(17).

$$R_{sb}^2 + R_{bs}^2 = 2R_d^2 + 2R_d c(\tau_3 + \tau_4) + c^2(\tau_3^2 + \tau_4^2) \tag{17}$$

The left of the Eq.(17) could also be written as Eq.(18) with Eq.(13) and Eq.(14).

$$R_{sb}^2 + R_{bs}^2 = 2H_h^2 + \left[2H_S + (H_t - H_r)\right]^2 + \left[2H_S - (H_t - H_r)\right]^2 \tag{18}$$

Plus the square of Eq.(15) and the square of Eq.(16), we could have Eq.(19).

$$H_h^2 + (H_t - H_r)^2 = R_d^2 \tag{19}$$

From Eq.(17), Eq.(18) and Eq.(19), R_d could be estimated by Eq.(20)

$$R_d = \frac{8H_S^2 - c^2(\tau_3^2 + \tau_4^2)}{2c(\tau_3 + \tau_4)} \tag{20}$$

Subtract the square of Eq.(11) from the square of Eq.(12), we could have Eq.(21).

$$R_{bs}^2 - R_{sb}^2 = 2R_d c(\tau_4 - \tau_3) + c^2(\tau_4^2 - \tau_3^2) \tag{21}$$

Eq.(21) could also be written as Eq.(22) by subtracting Eq.(14) from Eq.(12).

$$R_{bs}^2 - R_{sb}^2 = 8H_S H_r - 8H_S H_t \tag{22}$$

From Eq.(20), Eq.(21) and Eq.(22), H_t could be estimated by Eq.(23)

$$H_t = H_r - \frac{(\tau_4 - \tau_3)(c^2\tau_3\tau_4 + 4H_S^2)}{4H_S(\tau_3 + \tau_4)} \tag{23}$$

Eq.(20) and Eq.(23) are the localization solutions of the twice-reflection paths situations. This method is called DSBBS method in this paper.

2.2 Localization Performance Analysis

From Eq.(9), Eq.(10), Eq.(20) and Eq.(23), the estimation precision of R_d and H_t depend on the time differences between reflection paths and direct path. In this paper, the error propagation model is used to calculate the deviation of the estimators. If $f(x,y)$ is the function of variable x and y, the deviation of $f(x,y)$ could be written as Eq.(24).

$$\delta_f = \left|\frac{\partial f(x,y)}{\partial x}\right|\delta_x + \left|\frac{\partial f(x,y)}{\partial y}\right|\delta_y \tag{24}$$

For DSB method, R_d and H_t are all functions of τ_1 and τ_2. Therefore, by using Eq.(24), the deviations of DSB method could be written as:

$$\delta_{R_d} = \left|\frac{\partial R_d(\tau_1,\tau_2)}{\partial \tau_1}\right|\delta_{\tau_1} + \left|\frac{\partial R_d(\tau_1,\tau_2)}{\partial \tau_2}\right|\delta_{\tau_2} \tag{25}$$

$$\delta_{H_t} = \left|\frac{\partial H_t(\tau_1,\tau_2)}{\partial \tau_1}\right|\delta_{\tau_1} + \left|\frac{\partial H_t(\tau_1,\tau_2)}{\partial \tau_2}\right|\delta_{\tau_2} \tag{26}$$

where

$$\frac{\partial R_d}{\partial \tau_1} = \frac{c^2 D_2(D_1\tau_2^2 - D_2\tau_1^2 - 2D_1\tau_1\tau_2) - D_1 D_2^2(D_1 + D_2)}{2c(D_1\tau_2 + D_2\tau_1)^2} \tag{27}$$

$$\frac{\partial R_d}{\partial \tau_2} = \frac{c^2 D_1(D_2\tau_1^2 - D_1\tau_2^2 - 2D_2\tau_1\tau_2) - D_1^2 D_2(D_1 + D_2)}{2c(D_1\tau_2 + D_2\tau_1)^2} \tag{28}$$

$$\frac{\partial H_t}{\partial \tau_1} = \frac{D_1 D_2(D_1 + D_2)\tau_2 - c^2[(\tau_2^2 - 2\tau_1\tau_2)(D_1\tau_2 + D_2\tau_1) - D_2\tau_1\tau_2(\tau_2 - \tau_1)]}{2(D_1\tau_2 + D_2\tau_1)^2} \tag{29}$$

$$\frac{\partial H_t}{\partial \tau_2} = -\frac{D_1 D_2(D_1 + D_2)\tau_1 + c^2[(2\tau_1\tau_2 - \tau_1^2)(D_1\tau_2 + D_2\tau_1) - D_1\tau_1\tau_2(\tau_2 - \tau_1)]}{2(D_1\tau_2 + D_2\tau_1)^2} \tag{30}$$

For DSBBS method, R_d and H_t are all functions of τ_3 and τ_4. Therefore, by using Eq.(24), the deviations of DSBBS method could be written as:

$$\delta_{R_d} = \left|\frac{\partial R_d(\tau_3,\tau_4)}{\partial \tau_3}\right|\delta_{\tau_3} + \left|\frac{\partial R_d(\tau_3,\tau_4)}{\partial \tau_4}\right|\delta_{\tau_4} \tag{31}$$

$$\delta_{H_t} = \left|\frac{\partial H_t(\tau_3,\tau_4)}{\partial \tau_3}\right|\delta_{\tau_3} + \left|\frac{\partial H_t(\tau_3,\tau_4)}{\partial \tau_4}\right|\delta_{\tau_4} \tag{32}$$

where

$$\frac{\partial R_d}{\partial \tau_3} = \frac{c^2\left(\tau_3^2 + \tau_4^2\right) - 2c^2\tau_3(\tau_3 + \tau_4) - 8H_s^2}{2c(\tau_3 + \tau_4)^2} \tag{33}$$

$$\frac{\partial R_d}{\partial \tau_4} = \frac{c^2\left(\tau_3^2 + \tau_4^2\right) - 2c^2\tau_4(\tau_3 + \tau_4) - 8H_s^2}{2c(\tau_3 + \tau_4)^2} \tag{34}$$

$$\frac{\partial H_t}{\partial \tau_3} = \frac{8H_s^2\tau_4 - c^2(\tau_4^3 - \tau_3^2\tau_4 - 2\tau_3\tau_4^2)}{4H_s(\tau_3 + \tau_4)^2} \tag{35}$$

$$\frac{\partial H_t}{\partial \tau_4} = -\frac{8H_s^2\tau_3 + c^2(2\tau_3^2\tau_4 + \tau_3\tau_4^2 - \tau_3^3)}{4H_s(\tau_3 + \tau_4)^2} \tag{36}$$

Figure 3 shows the range and depth estimation deviations with different time delay errors of DSB method. Figure 4 shows the range and depth estimation deviations with different time delay errors of DSBBS method. From Figure 3 and Figure 4, it could be seen that the estimation deviations arises with the rising of source ranges and time delay estimation errors. And the estimation deviations of DSBBS method are less than that of the DSB method.

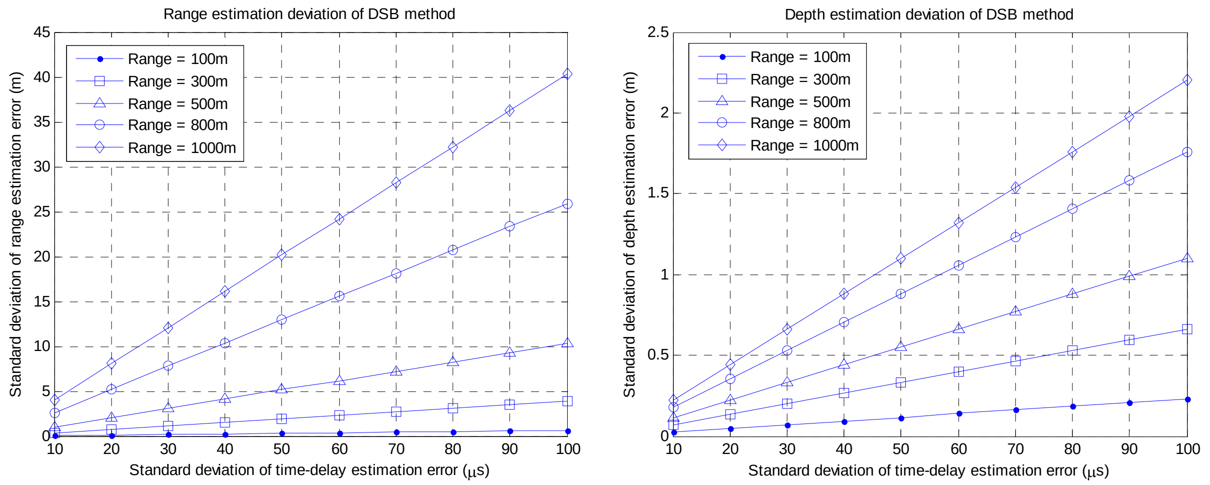

(a) Range deviation (b) Depth deviation

Figure 3 – Range and depth deviation of DSB method

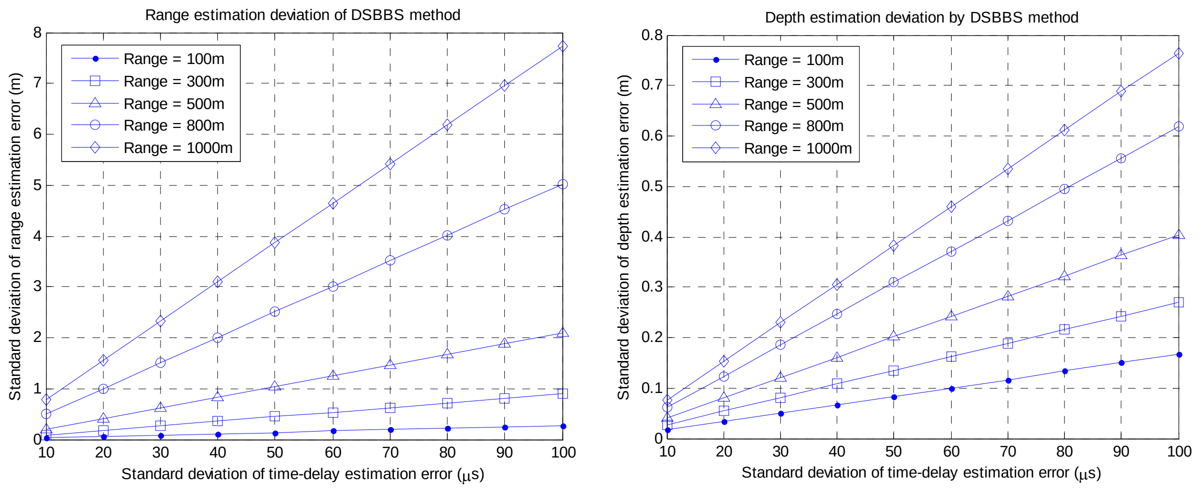

(a) Range deviation (b) Depth deviation

Figure 4 – Range and depth deviation of DSBBS method

3. SIMULATION RESULTS IN TYPICAL WAVEGUIDES

Generally, the time delay difference is estimated by cross-correlation processing. But in a multipath channel, there are numerous peaks in the cross-correlation function of two received signals. A better choice is the cepstrum method (11). The cepstrum of received signal is the sum of the cepstrum of source signal and the cepstrum of channel function. We can separate the channel function from received signal by cepstral processing. If the channel has several paths, the positions of peaks in the cepstrum will be defined by the arrival time delay differences between paths, so we can extract surface or bottom delay from cepstrum. In this paper, the cepstral processing is used to estimate the time differences between direct path and reflection paths.

In this section, the range and depth estimation deviations are analyzed by computer simulations in two typical waveguides. One is the Pekeris waveguide, which has a constant sound speed profile in the water. Another is a shallow sea waveguide, which has a thermocline with the thickness about 10m.

3.1 Localization Performance in Pekeris Waveguide

First, the Pekeris waveguide (12) is studied. The simulation geometry is depicted in Figure 5. The waveguide depth D is 100m, the sound speed in the water c is 1500m/s, the density of the water ρ is 1000kg/m^3, the sound speed in the bottom c_b is 2000m/s and the density of the bottom ρ_b is 1000kg/m^3.

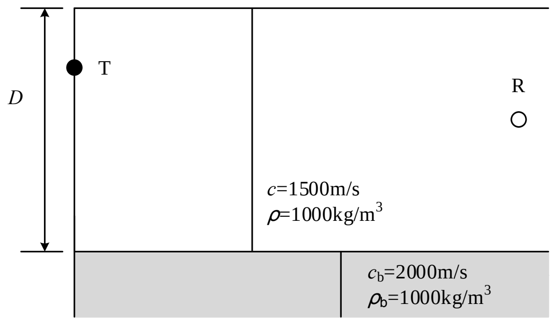

Figure 5 –Schematic of the Pekeris waveguide

Since the sound speed in the Pekeris waveguide is constant, the sound ray will travel in straight lines. The geometrical relationship between the direct path and reflection paths will comply with Eq.(9), Eq.(10), Eq.(20) and Eq.(23). Figure 6 shows the cepstrum of the signals received by a single hydrophone with the source range from 200m to 1km. The channel function is calculated using Bellhop model.

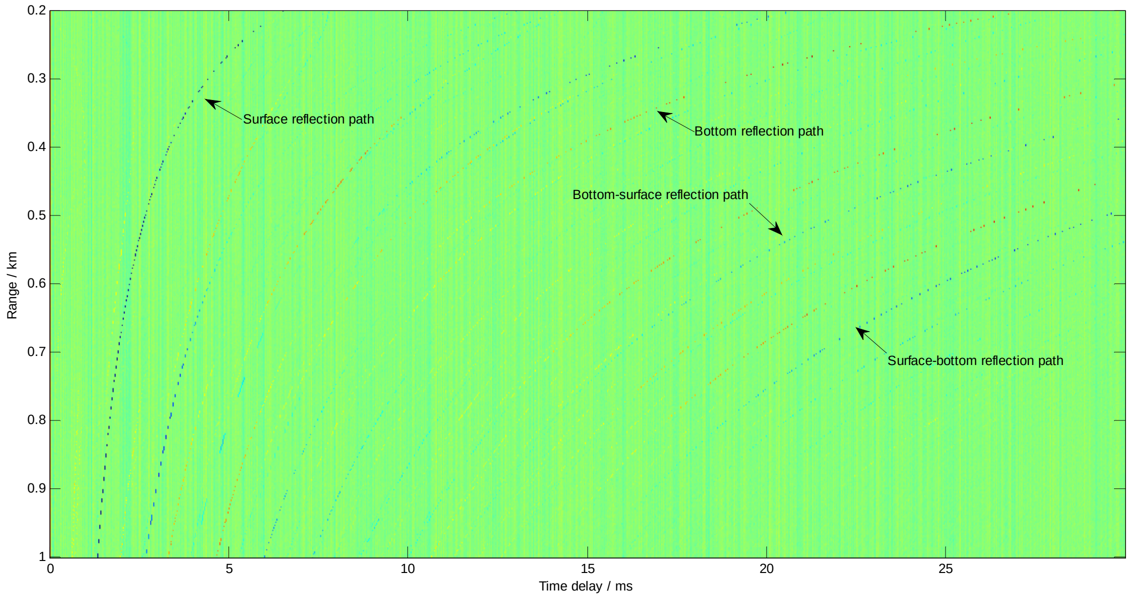

Figure 6 –Signal cepstrum in Pekeris waveguide

Figure 7 shows the range and depth estimation results by DSB method and DSBBS method. From the figure, it could be seen that the DSB method results become unstable at the source range about 600m, while the DSBBS method could give stable range and depth estimation more than 800m. With the increase of source range, the DSBBS estimation results show some fluctuations because of the instability of reflection paths.

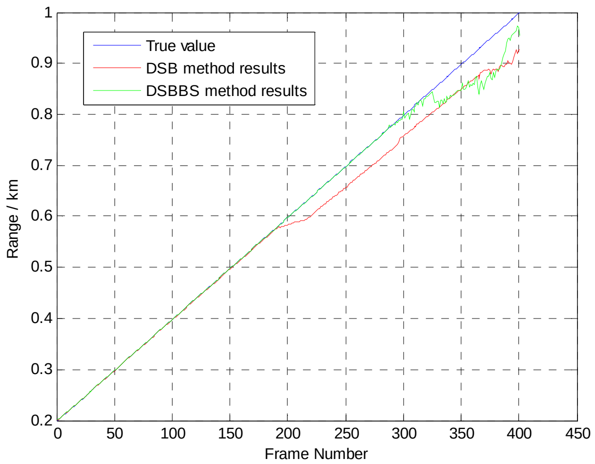

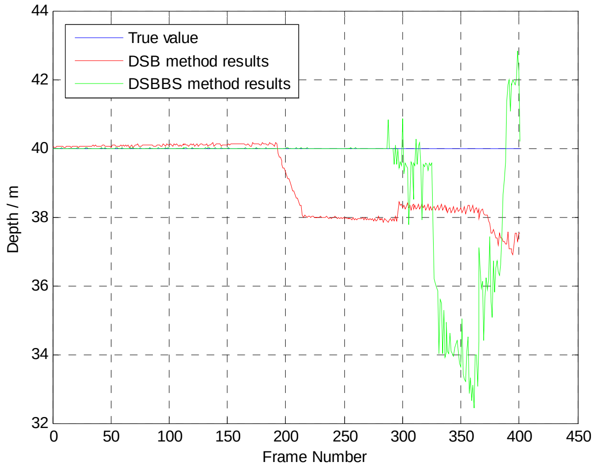

(a) Range estimation results (b) Depth estimation results

Figure 7 –Range and depth estimation results in Pekeris waveguide

3.2 Localization Performance in Shallow Sea Waveguide

Then, the shallow sea waveguide is studied. The sound speed profile is shown in Figure 8, which is measured in a sea trial. There is a thermocline from 45m to 55 m, and the sound speed decrease from 1526.6m/s to 1522.6m/s.

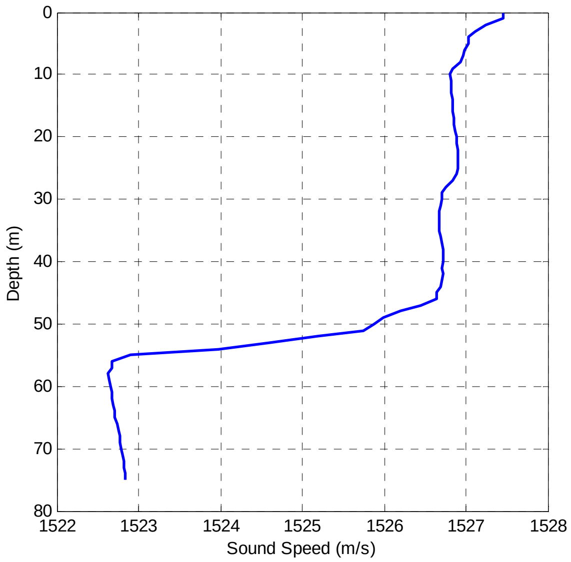

Figure 8 –Sound speed profile

Unlike Pekeris waveguide, the sound ray would travel along a curved path in the shallow sea waveguide. However, the range and depth estimation equations are derived in an isovelocity waveguide. In a speed-varying waveguide, sound ray warping would introduce errors to Eq.(9), Eq.(10), Eq.(20) and Eq.(23). Figure 9 shows the cepstrum of the signals received by a single hydrophone with the source range from 200m to 1km in the shallow sea waveguide.

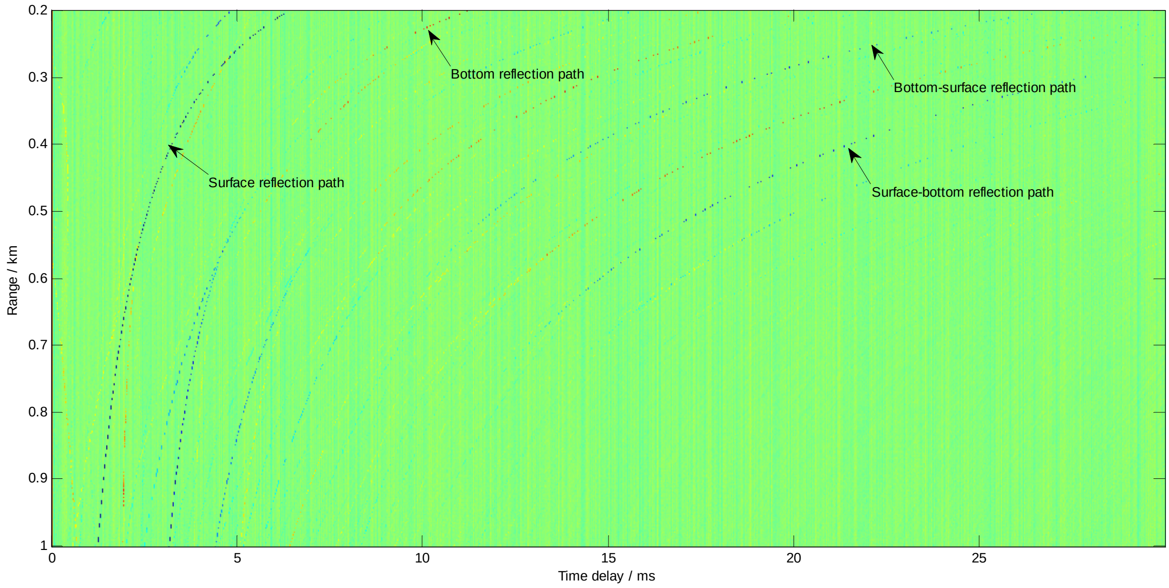

Figure 9 –Signal cepstrum in shallow sea waveguide

Figure 10 shows the range and depth estimation results by DSB method and DSBBS method. From the figure, it could be seen that both DSB and DSBBS method suffer degraded performance. But, the DSBBS method is still more robust that the DSB method.

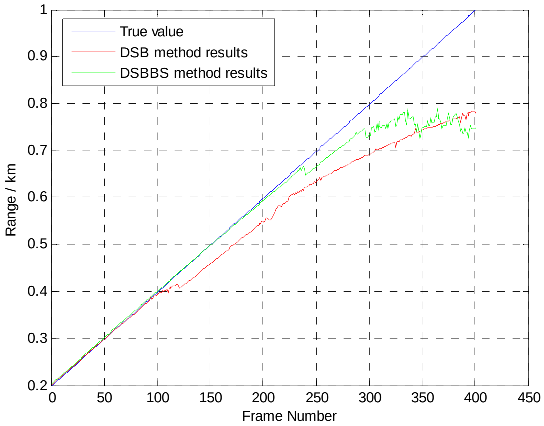

(a) Range estimation results

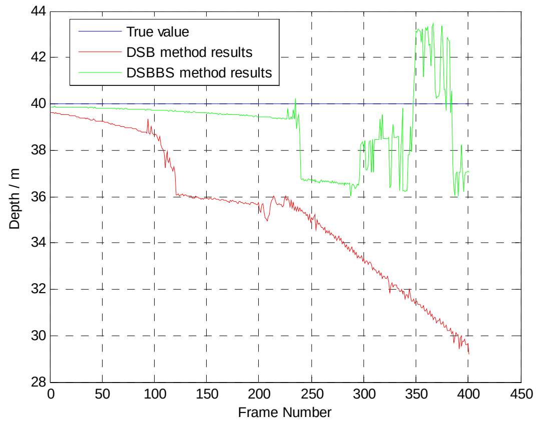

(b) Depth estimation results

Figure 10 –Range and depth estimation results in shallow sea waveguide

4. CONCLUSIONS

A new acoustic passive localization method for underwater targets in shallow water waveguide using homomorphic signal processing, called DSBBS method, is presented in this paper. The source range and depth are estimated by the time-delay differences between direct path and surface-bottom reflected path as well as bottom-surface reflected path. The estimation performance was compared with that of DSB method by computer simulation. Results show that the new method in this paper is more robust to time-delay estimation error and sound ray warping.

ACKNOWLEDGEMENTS

The authors appreciate the dedicated collaboration of Li Xuejian and Zhang Cheng in computer simulations. This work is supported by National Science Fund of China under Grant No. 11104029.

REFERENCES

1. Hinich MJ. Maximum-likelihood signal processing for a vertical array. J Acoust Soc Am. 1973; 54(2): 499–503.
2. Bucker HP. Use of calculated sound fields and matched-field detection to locate sound sources in shallow water. J Acoust Soc Am. 1976; 59(2): 368–373.
3. Abel JS, Smith JO. The spherical interpolation method for closed-form passive source localization using range difference measurements. Proc IEEE ICASSP; 6-9 April 1987; Dallas, USA 1987; p.471-474.
4. Nardone SC, Lindgren AG, Gong KE. Fundamental properties and performance of conventional bearings-only tracking. IEEE Transactions on Automatic Control, 1984; 29(9): 775-787.
5. Passerieux JM, Pillon D, Blanc-Benon P et al. Target motion analysis with bearing and frequency measurement. Proc 22nd Asilomar Conference on Signals, Systems, and Computers; 31 Oct 31-2 Nov, 1988; Pacific Grove, USA 1988; p.458 – 462.
6. Lee YP. Time-domain single hydrophone localization in a real shallow water environment. Proc IEEE OCEANS '98 Conference; 28 Sep-1 Oct 1998; Nice, France 1998. p.1074 - 1077.
7. Touz´e GL, Torras J, Nicolas B, et al. Source localization on a single hydrophone. Proc IEEE OCEANS '08 Conference; 15-18 Sept 2008; Quebec City, Canada 2008. p.1-6.
8. Jesus SM, Porter MB, Stéphan Y et al. Single hydrophone source localization. IEEE Journal of Oceanic Engineering. 2000; 25(3): 337-346.
9. Tao HL, Hickman G, Krolik JL et al. Single hydrophone passive localization of transiting acoustic sources. Proc IEEE OCEANS '07 Conference; 18-21 June 2007; Aberdeen, UK 2007. p.1-3.
10. Wu GQ. Estimation of range and depth of a submerged moving object by using noise cepstrum. Journal of Sound and Vibration. 2001; 245(5): 835-843.
11. Chen LJ, Gao X, An L. Multipath passive localization in shallow water channel. Journal of Nanjing University (Nature Science). 2012; 48(5): 609-615.
12. Jensen FB, Kuperman WA, Porter MB et al. Computational Ocean Acoustics. 2nd ed. New York USA: Springer Dordrecht Heidelberg London; 2011. P.345-356.